# Contact percolation transition in athermal particulate systems

Tianqi Shen,[1] Corey S. O'Hern,[1,2] and M. D. Shattuck[3]
[1]*Department of Physics, Yale University, New Haven, Connecticut 06520-8120, USA*
[2]*Department of Mechanical Engineering and Materials Science, Yale University, New Haven, Connecticut 06520-8286, USA*
[3]*Benjamin Levich Institute and Physics Department, The City College of the City University of New York, New York, New York 10031, USA*
(Received 3 October 2011; revised manuscript received 11 November 2011; published 27 January 2012)

Typical quasistatic compression algorithms for generating jammed packings of purely repulsive, frictionless particles begin with dilute configurations and then apply successive compressions with the relaxation of the elastic energy allowed between each compression step. It is well known that during isotropic compression these systems undergo a first-order-like jamming transition at packing fraction $\phi_J$ from an unjammed state with zero pressure and no force-bearing contacts to a jammed, rigid state with nonzero pressure, a percolating network of force-bearing contacts, and contact number $z = 2d$, where $d$ is the spatial dimension. Using computer simulations of two-dimensional systems with monodisperse and bidisperse particle size distributions, we investigate the second-order-like contact percolation transition, which precedes the jamming transition with $\phi_P < \phi_J$ and signals the formation of a system-spanning cluster of non-force-bearing contacts between particles. By measuring the number of nonfloppy modes of the dynamical matrix, the displacement field between successive compression steps, and the overlap between the adjacency matrix, which represents the network of contacting grains, at $\phi$ and $\phi_J$, we find that the contact percolation transition also signals the onset of a nontrivial mechanical response to applied stress. Our results show that cooperative particle motion occurs in unjammed systems significantly below the jamming transition for $\phi_P < \phi < \phi_J$, not only for jammed systems with $\phi > \phi_J$.

DOI: 10.1103/PhysRevE.85.011308 PACS number(s): 83.80.Fg, 64.60.ah, 61.43.Gt

## I. INTRODUCTION

The jamming transition in athermal [1], purely repulsive particulate systems, such as granular media, foams [2], colloidal microgel particles [3], and emulsions [4] has been characterized extensively in computer simulations [5] and experiments [6]. For example, when model frictionless spheres are compressed to packing fractions above $\phi_J$, static particle configurations undergo a first-order-like transition from an unjammed state at zero pressure and no force-bearing contacts between particles to a jammed state with nonzero pressure (and elastic energy), a rigid backbone of force-bearing contacts that spans the system, no nontrivial zero eigenmodes [7] of the dynamical matrix, and nonzero contact number $z = 2d$. Signatures of the jamming transition, such as anomalous scaling of the zero-frequency shear modulus with packing fraction [8] and diverging length scales [9,10] associated with cooperative particle rearrangements, have been investigated in thermal systems [3] in the zero-temperature limit and in sheared systems [11–14] in the zero-shear rate limit, but mainly for packing fractions near and above $\phi_J$.

However, there have been few detailed studies of the structural and mechanical properties of *unjammed* athermal particulate systems well below $\phi_J$. As shown in Fig. 1, typical quasistatic compression algorithms used to generate static packings in experiments start with a dilute collection of particles, and the sample is successively compressed by small amounts with energy relaxation allowed between each compression step. For $\phi < \phi_J$, the configurations are not completely rigid, and thus at long times after each small compression, particles can rearrange until all interparticle forces are zero. Despite this, particle motion in unjammed systems that occurs in response to compression and other perturbations can be highly heterogeneous, cooperative, and nonaffine at packing fractions well below $\phi_J$.

In this paper, we describe computational studies of a novel second-order-like transition (the contact percolation transition at $\phi_P$) in athermal particulate systems of purely repulsive, frictionless disks that signals the formation of a system-spanning cluster of connected non-force-bearing interparticle contacts and the onset of a nontrivial response to applied stress well below the jamming transition. These systems display robust power-law scaling behavior near $\phi_P$, but with a correlation length exponent that differs from the corresponding values for random continuum [16] and rigidity percolation [17]. In addition, we find that the number of "blocked" degrees of freedom, the accumulated particle displacements between successive compressions, and the overlap between the contact networks of the configurations at $\phi$ and $\phi_J$ begin to increase significantly near $\phi_P$. These results, which hold for both bidisperse and monodisperse particle size distributions, emphasize that the cooperative and nonaffine response to applied stress occurs in athermal particulate systems significantly below the jamming transition, not only for jammed systems with $\phi > \phi_J$ as has been emphasized in previous work.

## II. METHODS

We focus on systems composed of frictionless disks in two dimensions (2D) that interact via the purely repulsive linear spring potential

$$V(r_{ij}) = \frac{\epsilon}{2}\left(1 - \frac{r_{ij}}{\sigma_{ij}}\right)^2 \Theta\left(1 - \frac{r_{ij}}{\sigma_{ij}}\right), \qquad (1)$$

where $\epsilon$ is the characteristic energy scale, $\theta(x)$ is the Heaviside step function, $r_{ij}$ is the separation between the centers of disks $i$ and $j$, and $\sigma_{ij} = (\sigma_i + \sigma_j)/2$ is their average diameter. We studied systems with either monodisperse or bidisperse (50–50 by number of large and small disks with diameter ratio $\sigma_l/\sigma_s =$

 

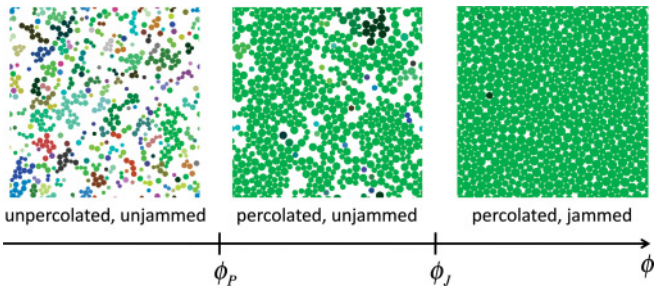


FIG. 1. (Color online) Typical snapshots from the quasistatic isotropic compression algorithm to generate static particle configurations as a function of packing fraction $\phi$. Particles with a given shading belong to the same cluster of mutually contacting particles. For (left) $\phi < \phi_P$, the system is unjammed, and the largest cluster of contacting particles does not percolate. The largest cluster begins to percolate for (middle) $\phi_P < \phi < \phi_J$, but the system remains unjammed since it possesses nontrivial zero-frequency (floppy) modes of the dynamical matrix and the interparticle forces at each contact are zero. For (right) $\phi > \phi_J$, the system is jammed with a percolating cluster of contacting particles that is rigid except for a small number of rattlers [15] and nonzero interparticle forces at each contact.

1.4 [5]) particle size distributions and system sizes in the range $N = 100$ to 6400 and implemented periodic boundary conditions in a unit square. We employed a quasistatic isotropic compression algorithm to generate static packings over a range of packing fractions [18]. We initialize each system with random particle positions at $\phi = 0$ and zero velocities. We then compress the system in steps of $\Delta\phi = 10^{-3}$ and relax the small particle overlaps after each step by solving Newton's equations of motion in the overdamped limit

$$m\vec{a}_i = \sum_j \vec{F}(r_{ij}) - b\vec{v}_i, \tag{2}$$

where $m$ and $\vec{a}_i$ are the particle mass and acceleration, $\vec{F}(r_{ij}) = -dV(r_{ij})/dr_{ij}\hat{r}_{ij}$, $\hat{r}_{ij}$ is the unit vector connecting the centers of particles $i$ and $j$, and $\tilde{b} = b\sigma_s/\sqrt{m\epsilon}$ is the damping coefficient, until the total potential energy per particle falls below a specified (extremely low) tolerance $V/\epsilon N < V_{\rm tol} = 10^{-16}$. We continue compression steps followed by relaxation until the systems jam at a configuration dependent $\phi_J$. The ensemble-averaged values for jamming onset in 2D are $\phi_J \approx 0.84$ [5] and 0.89 [19] in the overdamped and large-system limits for bidisperse and monodisperse particle size distributions, respectively. We verified that our results for the structural and mechanical properties near $\phi_P$ are independent of the particle size distribution, compression step for $\Delta\phi \leqslant 5 \times 10^{-3}$, and damping coefficient for $\tilde{b} \geqslant 1$.

## III. RESULTS

In Fig. 2, we characterize the contact percolation transition by plotting the probability $P(\phi)$ that the system forms a system-spanning network of interparticle contacts in either the $x$ or $y$ direction, where contact is determined by $r_{ij} \leqslant \sigma_{ij}$, at each $\phi$ immediately following a compression step. We note that the shape of $P(\phi)$ does not depend on whether the particle size distribution is monodisperse or bidisperse. We find that the contact percolation transition at $\phi_P = 0.549 < \phi_J$

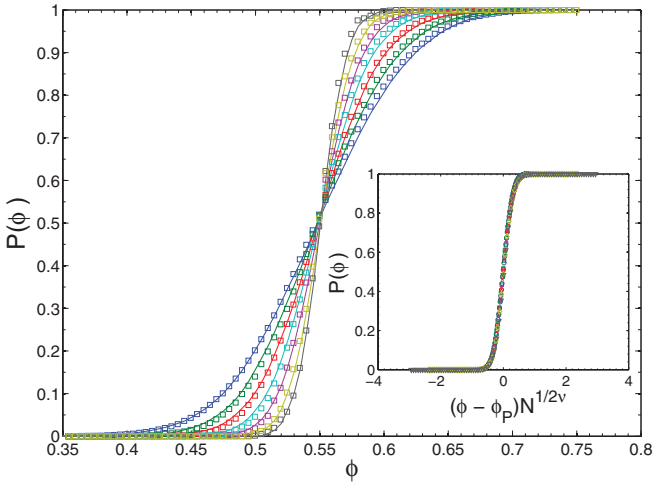


FIG. 2. (Color online) Percolation probability $P(\phi)$ that the system possesses a system-spanning cluster (in either the $x$- or $y$-direction) immediately following a compression step $\Delta\phi = 10^{-3}$ versus packing fraction $\phi$ for $N = 100$, 200, 400, 800, 1600, 3200, and 6400 particles (from bottom left to right) averaged over 400 configurations for bidisperse (lines) and monodisperse (squares) particle size distributions. Inset: Same as the main figure for the bidisperse systems except the horizontal axis is scaled by $(\phi - \phi_P)N^{1/2\nu}$, where $\phi_P = 0.549 \pm 0.001$ and $\nu = 1.68 \pm 0.08$.

becomes sharper with system size and obeys finite-size scaling, but with a correlation length exponent $\nu \approx 1.68$ [20] that is significantly larger than that for random continuum [16] and rigidity percolation [17], but smaller than that found for contact percolation in athermal particulate systems with short-range attractions [21]. (Note that percolation onset occurs at a similar value $\phi_P = 0.558 \pm 0.008$ for athermal systems with short-range attractions.) In contrast, the exponent $\tau \approx 2.01$ that characterizes the power-law scaling of the cluster size distribution and the fractal dimension $D \approx 1.89$ are similar to that for random continuum percolation and contact percolation for athermal systems with short-range attractions, and obey hyperscaling $D(\tau - 1) = 2$ (see Table I).

We have shown that immediately following a compression step, a system-spanning cluster of interparticle contacts forms at $t = 0$ for $\phi \geqslant \phi_P$, much below $\phi_J$. To determine if this geometrical transition influences the mechanical properties of the system, we measured (1) the eigenvalues of the dynamical matrix following relaxation and (2) the overlap of the adjacency matrix of configurations at $\phi$ and $\phi_J$. As static packings are compressed, they progressively become less floppy, (i.e., fewer single and collective particle motions

TABLE I. Critical exponents for contact percolation in athermal systems with purely repulsive interactions and short-range attractive interactions [21], as well as random continuum percolation [16] in 2D.

| Percolation type | $\nu$ | $\tau$ | $D$ |
|---|---|---|---|
| Repulsive contact | $1.68 \pm 0.08$ | $2.01 \pm 0.04$ | $1.89 \pm 0.03$ |
| Attractive contact | $1.92 \pm 0.03$ | $2.04 \pm 0.04$ | $1.88 \pm 0.04$ |
| Continuum | $1.34 \pm 0.02$ | $2.02 \pm 0.03$ | $1.91 \pm 0.04$ |

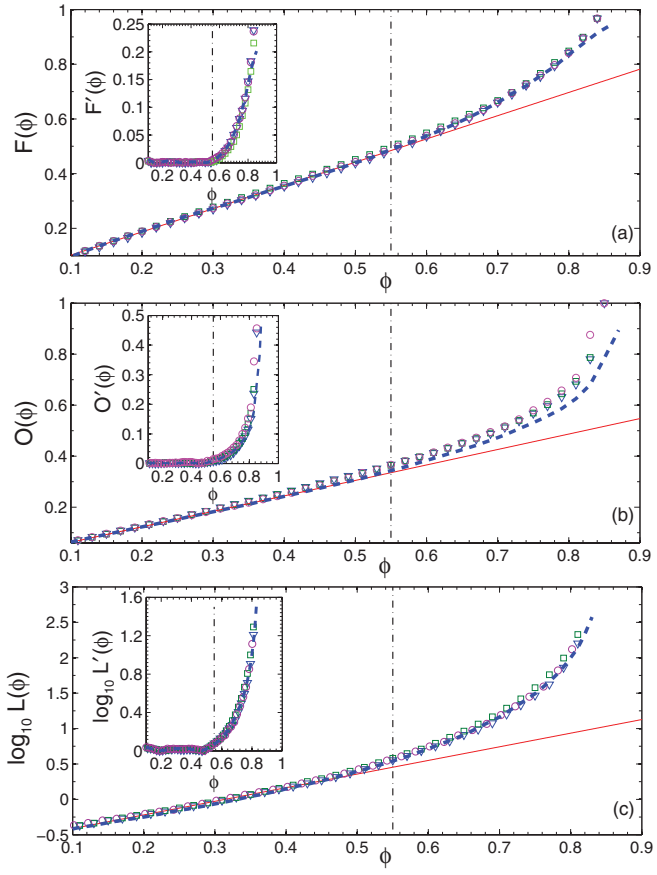


FIG. 3. (Color online) (a) The fraction $F(\phi)$ of nonfloppy eigenmodes of the dynamical matrix in the system measured following relaxation over a range of packing fractions for $\Delta\phi = 5 \times 10^{-3}$ and $N = 200$ (triangles), $\Delta\phi = 5 \times 10^{-3}$ and $N = 1000$ (squares), and $\Delta\phi = 10^{-3}$ and $N = 200$ (circles). The inset shows $F'(\phi) = F(\phi) - A\phi$ with $A \approx 0.85$. (b) The overlap $O(\phi)$ between the adjacency matrices at $\phi$ and $\phi_J$ immediately after a compression step for $\Delta\phi = 10^{-2}$ and $N = 200$ (triangles), $\Delta\phi = 10^{-2}$ and $N = 800$ (squares), and $\Delta\phi = 10^{-3}$ and $N = 200$ (circles). The inset shows $O'(\phi) = O(\phi) - B\phi$, where $B \approx 0.7$. (c) The logarithm (base 10) of the accumulated distance $L$ between successive compressions normalized by $\Delta\phi$ as a function of packing fraction for $\phi > 0.1$, $\Delta\phi = 10^{-2}$ and $N = 400$ (triangles), $\Delta\phi = 10^{-2}$ and $N = 1600$ (squares), and $\Delta\phi = 2 \times 10^{-3}$ and $N = 400$ (circles). The inset shows $\log_{10} L'(\phi) = \log_{10} L(\phi) - C\phi$, where $C \approx 2$. In all panels, the solid line is a fit to the low-$\phi$ behavior and the dot-dashed vertical line indicates the percolation transition at $\phi_P = 0.549$. The symbols indicate results for bidisperse particle size distributions. Results for monodisperse disks with $\Delta\phi = 10^{-2}$ and $N = 200$ are indicated with dashed lines.

cost zero energy). We quantify the increase in rigidity by measuring the fraction of nonfloppy or "blocked" eigenmodes $F(\phi)$, the ratio of the number $N_{nf}$ of nonzero eigenvalues of the dynamical matrix to the total number of nontrivial modes $2N' - 2$ (where $N' = N - N_r$ and $N_r$ is the number of rattler particles at jamming [15]), following relaxation after each compression step over a range of packing fractions. With this definition, $F(\phi_J) = 1$. In Fig. 3(a), we show that the fraction of nonfloppy modes $F(\phi)$ grows linearly with $\phi$ for small $\phi$. However, $F(\phi)$ begins to deviate from linear behavior near $\phi_P$ (i.e., $F'(\phi) = F(\phi) - A\phi > 0$ for $\phi \gtrsim \phi_P$), which signals an acceleration in the number of blocked directions in configuration space near $\phi_P$. This result does not depend sensitively on $\Delta\phi$, $N$, and the particle size distribution as shown in Fig. 3(a).

The adjacency matrix with elements $A_{ij} = 1$ if particles $i$ and $j$ are in contact and 0 otherwise characterizes the contact network of static packings. By calculating the overlap of the adjacency matrices at $\phi$ and $\phi_J$, $O(\phi) = N_c^{-1} \sum_{i>j} A_{ij}(\phi) A_{ij}(\phi_J)$, where $N_c$ is the number of distinct contacts in the configuration at $\phi_J$ and $O(\phi_J) = 1$, we can determine at what $\phi$ the system forms a network of contacts that is similar to the one at jamming. In Fig. 3(b), we show that $O(\phi)$ (calculated immediately following a compression step) grows linearly at small $\phi$, but as with $F(\phi)$, $O(\phi)$ begins to deviate from from linear behavior near $\phi_P$ [i.e., $O'(\phi) = O(\phi) - B\phi > 0$ for $\phi \gtrsim \phi_P$]. Thus the particular network of particle contacts that is responsible for mechanical stability at $\phi_J$ begins to form near $\phi_P$. Again, the results for $O(\phi)$ are insensitive to $\Delta\phi$, $N$, and the particle size distribution, especially near $\phi_P$.

In addition, we have identified a signature in the particle displacements that signals the onset nontrivial response to isotropic compression near $\phi_P$. We measure the accumulated distance traveled in configuration space (normalized by $\Delta\phi$)

$$L = (\Delta\phi)^{-1} \int_0^\infty dt \sqrt{\sum_{i=1}^{N} \vec{v}_i^2(t)} \tag{3}$$

from $t = 0$ after each compression to the end of the energy relaxation. In Fig. 3(c), we show that $L$ grows roughly exponentially for small $\phi$, but begins to deviate from the low-$\phi$ behavior near (slightly below) $\phi_P$ (i.e., $\log_{10} L - C\phi > 0$ for $\phi \gtrsim \phi_P$). As found for $F(\phi)$ and $O(\phi)$, the accumulated distance is insensitive to $\Delta\phi$, $N$, and the particle size distribution. For $\phi \lesssim \phi_P$, the particles move mainly affinely in response to isotropic compression. In contrast, for $\phi \gtrsim \phi_P$ particles become blocked by their neighbors and must move cooperatively and in more circuitous routes to relax the applied stress. The blocked directions in configuration space correspond to the nonfloppy modes of the dynamical matrix. Thus, the contact percolation transition signals the onset of collective particle motion in athermal particulate systems subjected to isotropic compression.

## IV. CONCLUSION

A decade of work has emphasized the importance of the jamming transition that signals the onset of nonzero pressure, energy, and shear stress following relaxation at long times in systems of frictionless spherical particles [5]. This has caused a possible misconception in the literature that the onset of cooperative and spatially complex response to applied stress in athermal particulate media occurs at the jamming transition in the large-system limit, not below. Further, a number of studies have focused on the critical behavior of the shear stress, pressure, and other physical quantities in athermal systems of frictionless particles near jamming [11–14,22], but there have been very few studies of these properties well below jamming.

In this paper, we describe extensive computational studies of the geometrical and mechanical properties of *unjammed*, athermal systems of frictionless particles undergoing quasistatic isotropic compression below $\phi_J$. The importance of this work is that it reports that the onset of the nontrivial mechanical response of these systems to applied stress occurs at a new critical point (the contact percolation transition) well below the jamming transition. We believe that both experimental and computational studies of athermal particulate media, such as granular materials, compressed emulsions, and foams, well below jamming [23] (similar to those presented here) are important for understanding the protocol dependence of the probabilities with which static packings occur [18], irreversibility of particle motion under shear reversal [24], and frequency-dependent elastic moduli [25]. In future computational studies, we will investigate the similarities in the contact networks and other structural properties between unjammed frictionless packings above the percolation transition with $\phi_P < \phi < \phi_J$ and mechanically stable frictional packings in the same range of packing fraction.

## ACKNOWLEDGMENTS

This research was supported by the National Science Foundation under Grants No. DMS-0835742 (CO, TS), No. PHY-1019147 (TS), and No. CBET-0968013 (MS) and the Raymond and Beverly Sackler Institute for Biological, Physical, and Engineering Sciences (TS).

[1] In this context, athermal systems are those in which thermal fluctuations are negligible compared to other energy scales, and posses dissipation mechanisms that bring these systems to rest in the absence of driving forces.
[2] D. J. Durian, Phys. Rev. E **55**, 1739 (1997).
[3] Z. Zhang, N. Xu, D. T. N. Chen, P. Yunker, A. M. Alsayed, K. B. Aptowicz, P. Habdas, A. J. Liu, S. R. Nagel, and A. G. Yodh, Nature (London) **459**, 230 (2009).
[4] M.-D. Lacasse, G. S. Grest, D. Levine, T. G. Mason, and D. A. Weitz, Phys. Rev. Lett. **76**, 3448 (1996).
[5] C. S. O'Hern, L. E. Silbert, A. J. Liu, and S. R. Nagel, Phys. Rev. E **68**, 011306 (2003).
[6] T. S. Majmudar, M. Sperl, S. Luding, and R. P. Behringer, Phys. Rev. Lett. **98**, 058001 (2007).
[7] A. Tanguy, J. P. Wittmer, F. Leonforte, and J.-L. Barrat, Phys. Rev. B **66**, 174205 (2002).
[8] W. G. Ellenbroek, Z. Zeravcic, W. van Saarloos, and M. van Hecke, Europhys. Lett. **87**, 34004 (2009).
[9] J. A. Drocco, M. B. Hastings, C. J. Olson Reichhardt, and C. Reichhardt, Phys. Rev. Lett. **95**, 088001 (2005).
[10] L. E. Silbert, A. J. Liu, and S. R. Nagel, Phys. Rev. Lett. **95**, 098301 (2005).
[11] B. P. Tighe, E. Woldhuis, J. J. C. Remmers, W. van Saarloos, and M. van Hecke, Phys. Rev. Lett. **105**, 088303 (2010).
[12] C. Heussinger, L. Berthier, and J.-L. Barrat, Europhys. Lett. **90**, 20005 (2010).
[13] C. Heussinger and J.-L. Barrat, Phys. Rev. Lett. **102**, 218303 (2009).
[14] D. Vågberg, D. Valdez-Balderas, M. A. Moore, P. Olsson, and S. Teitel, Phys. Rev. E **83**, 030303(R) (2011).
[15] Jammed systems possess all positive nontrivial eigenvalues of the dynamical matrix except for $d$ zero eigenvalues per rattler particle with fewer than $d+1$ contacts, where $d$ is the spatial dimension.
[16] E. T. Gawlinski and H. G. Stanley, J. Phys. A: Math. Gen. **14**, L291 (1981).
[17] D. J. Jacobs and M. F. Thorpe, Phys. Rev. Lett. **75**, 4051 (1995).
[18] G.-J. Gao, J. Blawzdziewicz, and C. S. O'Hern, Phys. Rev. E **74**, 061304 (2006).
[19] A. Donev, S. Torquato, F. H. Stillinger, and R. Connelly, J. Appl. Phys. **95**, 989 (2004).
[20] The correlation length exponent $\nu \approx 1.68$ is similar to that reported for "force-bearing" contact percolation , see S. Ostojic, E. Somfai, and B. Nienhuis, Nature (London) **439**, 828 (2006).
[21] G. Lois, J. Blawzdziewicz, and C. S. O'Hern, Phys. Rev. Lett. **100**, 028001 (2008).
[22] P. Olsson and S. Teitel, Phys. Rev. Lett. **99**, 178001 (2007).
[23] M. M. Bandi, M. K. Rivera, F. Krzakala, and R. E. Ecke, e-print arXiv:0910.3008.
[24] S. Slotterback, M. Mailman, K. Ronaszegi, M. van Hecke, M. Girvan, and W. Losert, e-print arXiv:1109.5167.
[25] B. P. Tighe, Phys. Rev. Lett. **107**, 158303 (2011).